

Advantages and Disadvantages of Parameter Search Algorithms for Permittivity Estimation for Microwave Breast Imaging

Declan O’Loughlin*, Bárbara L. Oliveira, Martin Glavin, Edward Jones and Martin O’Halloran.

Electrical and Electronic Engineering, National University of Ireland Galway, Ireland.

*d.oloughlin4@nuigalway.ie

Abstract—Multiple clinical investigations of radar-based breast imaging devices have been demonstrated in recent years, including two competing commercial systems which are currently being tested in clinics. Ongoing trials include participants with both dense and non-dense breasts and the average dielectric properties of the breast can vary substantially with density. Numerous studies have shown that this normal variance in the dielectric properties of the breast between individuals can impact both the image quality and the expected sensitivity of radar-based breast imaging. This paper examines the potential to use parameter search algorithms to improve the sensitivity of radar-based breast imaging. Although these parameter search algorithms have been shown to improve image quality in a limited number of test cases, this is the first analysis of the potential impact of realistic dielectric properties estimation on the sensitivity of radar-based imaging.

I. INTRODUCTION

Radar-based breast imaging is an emerging imaging modality for the early detection of breast cancer [1], [2]. A number of clinical investigations of radar-based breast imaging systems have recently been published [3]–[8]. Two competing systems are being developed commercially: the MARIA[®] system by Micrima Ltd. (Bristol, the UK) which is undergoing trials with 994 participants [3]; and the Wavelia system by Microwave Vision SA (Villebon-sur-Yvette, France) which is being used in a pilot clinical investigation at the National University of Ireland Galway with 30 participants [9]. Particularly encouraging results have been demonstrated in dense breasts using MARIA[®], a known independent risk factor for breast cancer [3], [10]. Comprehensive reviews of these clinical studies and the other imaging systems used with human participants have been published [1], [11].

As research in radar-based imaging moves towards larger and larger clinical investigations, it is important to use imaging algorithms that are suitable for all women, regardless of breast composition. The breast varies substantially from individual to individual in terms of tissue composition, from very little fibrous and glandular tissues to as much as 50% by volume [12]. The breast tissue composition in terms of proportions of glandular tissue by volume is known to impact both the image quality and the sensitivity achievable with radar-based breast imaging [13], [14]. A number of methods to account for the variance in breast tissue composition have been proposed, however, most have only been tested in a limited number of simplified test-cases [15]–[19].

In this work, the sensitivity achieved using dielectric properties estimation algorithm is compared to the current state-of-the-art method, known as fixed-value estimation. Fixed-value estimation selects one estimate of the average dielectric properties of the breast for all test-cases, however, previous work has shown that the sensitivity can be impaired by errors in this estimate [14]. Parameter search algorithms are a promising approach for dielectric properties estimation for radar-based imaging, and have been tested using both experimental and clinical data [18], [19]. However, these studies have used a limited number of test cases and have primarily focused on the potential of parameter search algorithms to improve the image quality and have not considered the sensitivity. For the first time, this work examines the potential impact of parameter search algorithms on the sensitivity of radar-based imaging, whereas previous work using the same algorithm has looked only at image quality in a limited number of case studies [18].

The following section describes the methods including the experimental data set and the dielectric properties estimation algorithm. Section 3 describes the results, including the potential sensitivity that can be achieved, and the disadvantages of the dielectric properties estimation approach and Section 4 concludes this work.

II. METHODS

Fundamentally, radar-based imaging uses knowledge of propagation within the breast to “synthetically focus” backscattered signals to points in the imaging domain. As described in [18], a number of assumptions are required for practical implementation of a radar-based imaging algorithm. These assumptions can be divided into two main types:

- simplifying the imaging domain to a homogeneous layer with assumed dielectric properties;
- and using the same dielectric properties estimate for each individual breast (fixed-value estimate).

This work addresses the second assumption. Where previous work in [14] used idealised dielectric properties estimation algorithms to identify if the fixed-value estimate assumption affects the sensitivity, this work uses parameter search algorithms to identify suitable estimates without prior knowledge of the tumour location or dielectric properties of the breast.

The chosen parameter search algorithm was first proposed in [18] and was shown to be potentially suitable for

dielectric properties estimation. However, the algorithm was only tested in a limited number of case studies and only the image quality was quantified, not the sensitivity. In contrast, in this work, the same algorithm is used with a larger number of test cases and quantitative criteria are used to determine if the tumour was detected without knowledge of the tumour location. Based on these quantitative criteria, the sensitivity using both the realistic parameter search algorithm and the idealised fixed-value estimation method are compared.

A. Experimental Breast and Tumour Phantoms

The BRIGID phantoms contain diverse experimental test cases with a variety of tumour shapes and sizes and a range of breast densities and were used in this work to acquire the signals [20]. The breast and tumour phantoms model two types of variance:

- firstly, the normal and healthy variance in terms of the proportions of adipose and glandular tissues;
- and secondly, the variance in size and shape of breast tumours observed in clinical practice.

Examples of both the breast and tumour phantoms can be seen in Figure 1.

The normal variance of healthy tissue can be characterised in terms of volume of glandular fraction (VGF), or the proportion of the breast that contains glandular tissues [12]. Using advances in three-dimensional breast imaging, studies have suggested that the breast can contain between 0% and 50% VGF and over 90% of women in the study had VGF of 30% or below. The five BRIGID breast phantoms were used in this work contain between 0%, 10%, 15%, 20% and 30% VGF.

22 tumour phantoms which model both benign and malignant cases [20]. Benign tumours are characterized by spherical shape and smooth borders whereas malignant tumours are characterized by irregular shapes and spiculated borders [21]. The variety of tumour shapes used in this work helps assess the robustness of the parameter search algorithm to the substantial variance in tumour shape and size observed in clinical practice.

The breast and tumour phantoms and the fabrication process are described in detail in [20]. All four tissue types (skin, fat, gland and tumour) were made using polyurethane rubber combined with graphite and carbon black powders to control the dielectric properties. Once mixed, the rubber cures over a 16 to 24 hour period. The breast phantoms consist of a hemispherical skin which is, on average, 2 mm thick. Once cured, the skins were filled with conical structures modelling the breast lobes and the remainder of the breast phantom was filled with an adipose-mimicking material. For each phantom (with VGFs ranging from 0% to 30%), a hole was left so that each breast phantom could be combined with each tumour phantom.

Tumour-mimicking material was also manufactured from the same rubber-based mixture and the tumour shapes were moulded by hand prior to curing. The tumour shapes were created in line with the principles outlined in [22]. Once cured, each tumour was encased in the same adipose-mimicking material as the breast phantoms. Using each of

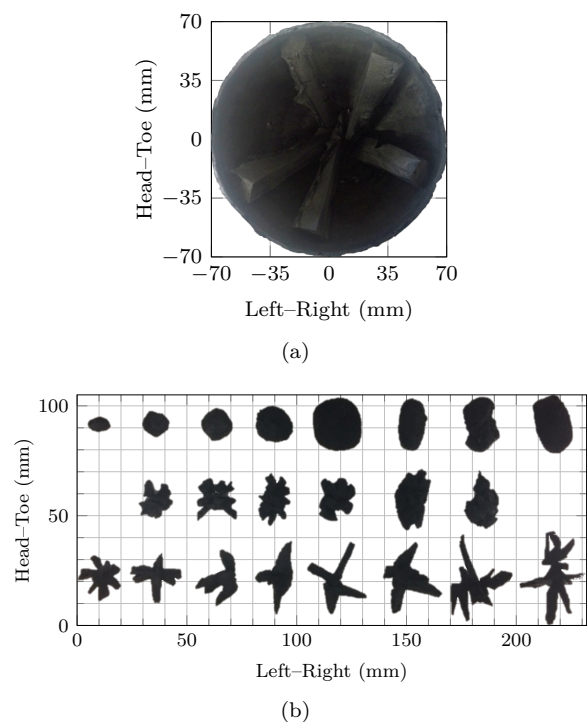


Fig. 1. An image of the interior of a breast phantom with 10% VGF is shown in (a). The conical glandular structures can be seen as well as the hemispherical 2 mm skin. The 22 tumour phantoms are shown in (b). Each tumour phantom can be used with each breast phantom for a total of 110 test scenarios.

the 22 tumour phantoms in combination with each of the five breast phantoms results in a total of 110 test cases.

B. Signal Acquisition and Imaging

Signal acquisition and imaging are described completely in [18]. Scattered signals were acquired using a Rohde and Schwartz ZNB40 vector network analyzer (VNA) and ZN-Z84 switching matrix. The phantoms were sequentially illuminated by 24 microstrip antennas equally spaced around a 7 cm radius hemispherical radome. The antennas were first described in [23] and were used with patients in [7]. The phantoms were illuminated by a stepped frequency sine wave at 51 linearly spaced frequency points between 2 GHz and 4 GHz.

To reduce the large skin reflection, rotational subtraction was used [24]. The “rotated” scan was acquired without any mechanical movement as the antenna array was designed to be rotationally symmetrical. After artefact removal, a set of images were reconstructed using average dielectric properties estimates between $8 \leq \epsilon_r \leq 13$, where the range of estimates was informed by the known dielectric properties of the breast phantoms. All images were reconstructed using multistatic Delay-and-Sum as in [14]. All data acquisition, artefact removal and imaging were completed in the frequency domain [25].

For each scan, 21 images were reconstructed at relative permittivity estimates linearly spaced between $8 < \epsilon_r < 14$. For each of the 21 images, the average of the absolute gradient of all points in the image was used to estimate the fitness of the image [26]. The image with the highest fitness was selected and the quantitative criteria described in this section were used to determine if a tumour was

TABLE I

THE PERMITTIVITY RANGES AND SENSITIVITY ACHIEVED USING THE PARAMETER SEARCH (PS) ALGORITHM WITH 22 TUMOUR MODELS IN 5 BREAST PHANTOMS OF INCREASING VGF. ALSO SHOWN ARE THE IDEALISED RESULTS USING THE SAME TEST CASES FROM [14] FOR FIXED-VALUE (FV) ESTIMATION, THE CURRENT STANDARD.

VGF	ε_r	PS	FV
0%	8–10.5	91%	91%
10%	8–9.75	77%	59%
15%	8–10.25	82%	86%
20%	8–13	73%	68%
30%	8–11	14%	18%
All	8–13	67%	65%

detected. The parameter search algorithm itself was first described in detail in [18].

The criteria used for tumour detection are described in detail in [14]. An image was considered a true positive if the main response in the image lay within the known physical extent of the tumour and the magnitude of the main response was 1.5 dB higher than the next strongest response in the image. Although the criteria were based on subjective image analysis, the criteria are one of the first attempts at quantitative analysis of tumour detection.

III. RESULTS

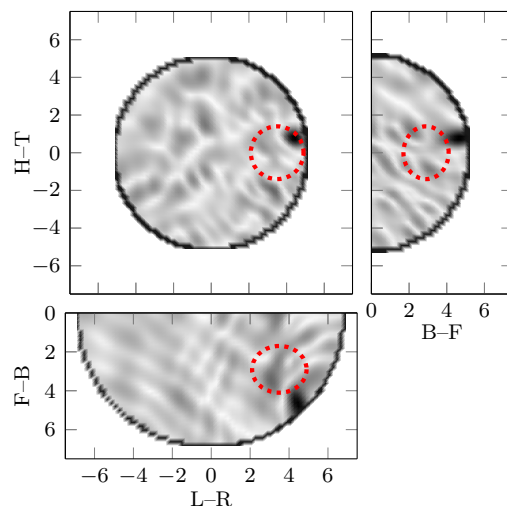
In this section, the sensitivity results from using the parameter search algorithms with the BRIGID phantoms are presented.

A. Overall Sensitivity Results

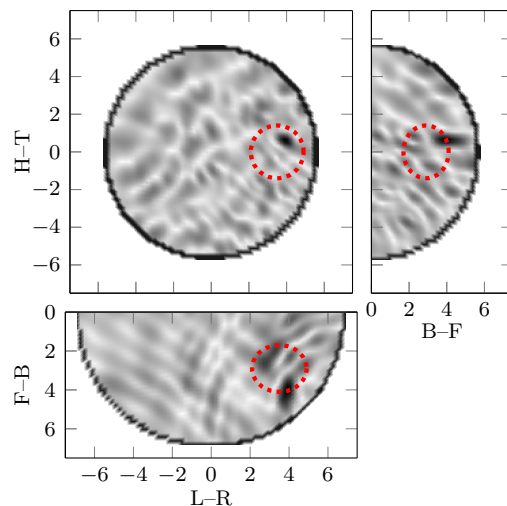
Firstly, the overall sensitivity achieved using the parameter search algorithm is presented in Table I. Also shown is the sensitivity using an idealised estimation method known as fixed-value estimation which is described in detail [14]. The fixed-value estimate is determined using *a priori* knowledge of the tumour location and chosen to optimise the sensitivity. In contrast, the parameter search estimates are chosen blind to the tumour location for each individual imaging scenario (i.e. 110 estimates were chosen for the 110 test cases).

Firstly, it can be observed from Table I that the sensitivity decreases as the VGF of the phantom increases. Only 14% of tumours were detected in a breast phantom with 30% VGF, which is consistent with previous experimental work such as [24], where high VGF was found to be the most challenging case for radar-based imaging. However, less than 50% of women have VGF of greater than 18% [12], suggesting that these difficult cases may be more rare than initially thought from density estimation from two-dimensional mammograms [27].

Secondly, sensitivity using the parameter search algorithm is slightly better overall compared to the idealised fixed-value estimate (67% compared to 65%). Most importantly, the parameter search algorithm used no *a priori* knowledge such as the dielectric properties of the breast phantoms or the tumour locations, whereas the fixed-value estimate was chosen to maximise the sensitivity. However, the sensitivity using fixed-value estimation depends greatly on the estimate used [14]. For example, for these test-cases, over-estimating the fixed-value estimate at $\varepsilon_r = 13$ instead



(a)



(b)

Fig. 2. Slices of maximum intensity with reference to the front (F), back (B), head (H), toe (T), left (L) and right (R) of the breast phantom. (a) is the image most highly rewarded by the parameter search algorithm whereas (b) is the optimal image selected by the idealised fixed-value estimation algorithm—reconstructed at $\varepsilon_r = 8.5$ and $\varepsilon_r = 10.25$ respectively. The parameter search algorithm prioritises the image with lower background energy although the image with higher background energy has lower localisation error.

of the optimal value of $\varepsilon_r = 10.25$ results in the sensitivity dropping to 41%.

Thirdly, worst-case sensitivity using the parameter search algorithm is better than worst-case sensitivity using fixed-value estimation. With the exception of the most dense phantom, the worst-case sensitivity using the parameter search algorithm is 73% compared to 59% for the idealised fixed-value estimate.

B. Errors due to parameter search

In this section, some potential errors due to the parameter search estimation algorithm are analysed. Two images reconstructed at $\varepsilon_r = 8.5$ and $\varepsilon_r = 10.5$ of tumour phantom 9 in a breast phantom with 15% VGF are shown in Figure 2. The image reconstructed at $\varepsilon_r = 8.5$ is

most highly rewarded by the parameter search algorithm. However, as can be seen in Figure 2a, the response in the image is very close to the skin and is not in the tumour area (shown by the red circle). In contrast, the image reconstructed at $\epsilon_r = 11.0$ is selected by the idealised fixed-value estimation and does show the tumour in the correct location.

For this particular imaging scenario, the parameter search algorithm rewards an image which less background energy but with the tumour response extremely close to the skin (Figure 2a and not Figure 2b). A similar trend was observed in [19] where a penalisation term for responses close to the borders of the imaging domain was introduced. These images suggest that care needs to be taken when defining the imaging domain such that artefacts close to the boundaries do not impair the dielectric properties estimation process.

IV. CONCLUSIONS

Previous work has demonstrated how the current state-of-the-art in radar-based imaging (fixed-value estimation) may not be suitable for imaging populations with a large variance in breast density. This work helps to show how a realistic parameter search algorithm can improve the sensitivity achieved with radar-based breast imaging in these diverse populations without any prior knowledge. While parameter search algorithms have previously been investigated in small numbers of case studies to investigate the suitability of the approach for dielectric properties estimation, the potential impact on sensitivity using radar-based imaging has not been considered.

This work demonstrates how dielectric properties estimation is useful in realistic test cases for selecting the optimal dielectric properties estimate for each imaging scenario. These results indicate that the parameter search algorithm used in this work can improve the worst-case sensitivity even when compared to an idealised fixed-value estimate chosen to maximise the overall sensitivity.

Additionally, these results highlight a potential issue with parameter search algorithms: artefacts can occur close to the boundaries of the imaging domain which can be highly rewarded by the parameter search algorithm. Future work is needed to carefully define the imaging domain to minimise the impact of this type of artefact and to develop penalisation terms to reduce the negative effects.

ACKNOWLEDGEMENTS

This work was supported by the Irish Research Council (Grant no. RCS1326), Science Foundation Ireland (Grant no. 12/IP/1523), the MiMED COST Action (TD1301) and the European Research Council under the European Union's Horizon-2020 Programme (H2020)/ERC grant agreement BioElecPro number 637780.

REFERENCES

- [1] D. O'Loughlin, M. O'Halloran, B. M. Moloney, *et al.*, "Microwave Breast Imaging: Clinical Advances and Remaining Challenges," *Transactions on Biomedical Engineering*, Feb. 2018.
- [2] J.-C. Bolomey, "Crossed Viewpoints on Microwave-Based Imaging for Medical Diagnosis: From Genesis to Earliest Clinical Outcomes," in *The World of Applied Electromagnetics*, A. Lakhtakia and C. M. Furse, Eds., Cham, Switzerland: Springer International Publishing, 2018, pp. 369–414.
- [3] A. W. Preece, I. J. Craddock, M. Shere, *et al.*, "MARIA M4: Clinical evaluation of a prototype ultra-wideband radar scanner for breast cancer detection," *Journal of Medical Imaging*, vol. 3, no. 3, p. 033 502, Jul. 2016.
- [4] E. C. Fear, J. Bourqui, C. F. Curtis, *et al.*, "Microwave Breast Imaging With a Monostatic Radar-Based System: A Study of Application to Patients," *IEEE Transactions on Microwave Theory and Techniques*, vol. 61, no. 5, pp. 2119–2128, May 2013.
- [5] F. Yang, L. Sun, Z. Hu, *et al.*, "A large-scale clinical trial of radar-based microwave breast imaging for Asian women: Phase I," in *Proceedings of the International Symposium on Antennas and Propagation (APSURSI)*, San Diego, CA, USA: IEEE, Jul. 9–14, 2017, pp. 781–783.
- [6] H. Song, S. Sasada, T. Kadoya, *et al.*, "Detectability of Breast Tumor by a Hand-held Impulse-Radar Detector: Performance Evaluation and Pilot Clinical Study," *Scientific Reports*, vol. 7, no. 1, Dec. 2017, Art. 16353.
- [7] E. Porter, M. Coates, and M. Popović, "An Early Clinical Study of Time-Domain Microwave Radar for Breast Health Monitoring," *IEEE Transactions on Biomedical Engineering*, vol. 63, no. 3, pp. 530–539, Mar. 2016.
- [8] Y. Kuwahara, "Microwave Imaging for Early Breast Cancer Detection," in *New Perspectives in Breast Imaging*, A. M. Malik, Ed., InTech, Oct. 2017.
- [9] A. Fasoula, L. Duchesne, J. Gil Cano, *et al.*, "On-Site Validation of a Microwave Breast Imaging System, before First Patient Study," *Diagnostics*, vol. 8, no. 3, p. 53, Aug. 2018.
- [10] N. Ridley, M. Shere, I. Lyburn, *et al.*, "Cancer detection in dense tissue using radiofrequency imaging—a clinical evaluation," in *Proceedings of the European Congress of Radiology Annual Meeting*, Vienna, Austria: European Society of Radiology, Mar. 1–5, 2017.
- [11] A. Modiri, S. Goudreau, A. Rahimi, *et al.*, "Review of Breast Screening: Towards Clinical Realization of Microwave Imaging," *Medical Physics*, vol. 44, no. 12, e446–e458, Nov. 2017.
- [12] S.-Y. Huang, J. M. Boone, K. Yang, *et al.*, "The characterization of breast anatomical metrics using dedicated breast CT," *Medical Physics*, vol. 38, no. 4, pp. 2180–2191, Apr. 1, 2011.
- [13] D. O'Loughlin, F. Krewer, M. Glavin, *et al.*, "Focal quality metrics for the objective evaluation of confocal microwave images," *International Journal of Microwave and Wireless Technologies*, vol. 9, no. 07, pp. 1365–1372, Sep. 2017.
- [14] D. O'Loughlin, B. L. Oliveira, A. Santorelli, *et al.*, "Sensitivity and specificity estimation using patient-specific microwave imaging in diverse experimental

- breast phantoms,” *IEEE Transactions on Medical Imaging*, Aug. 2018.
- [15] J. Bourqui and E. C. Fear, “System for Bulk Dielectric Permittivity Estimation of Breast Tissues at Microwave Frequencies,” *IEEE Transactions on Microwave Theory and Techniques*, vol. 64, no. 9, pp. 3001–3009, Sep. 2016.
- [16] M. Sarafianou, I. J. Craddock, T. Henriksson, *et al.*, “MUSIC processing for permittivity estimation in a Delay-and-Sum imaging system,” in *Proceedings of the 7th European Conference on Antennas and Propagation (EuCAP)*, Gothenburg, Sweden: IEEE, Apr. 8–12, 2013, pp. 839–842.
- [17] D. W. Winters, E. J. Bond, B. D. Van Veen, *et al.*, “Estimation of the Frequency-Dependent Average Dielectric Properties of Breast Tissue Using a Time-Domain Inverse Scattering Technique,” *IEEE Transactions on Antennas and Propagation*, vol. 54, no. 11, pp. 3517–3528, Nov. 2006.
- [18] D. O’Loughlin, B. L. Oliveira, M. A. Elahi, *et al.*, “Parameter Search Algorithms for Microwave Radar-Based Breast Imaging: Focal Quality Metrics as Fitness Functions,” *Sensors*, vol. 17, no. 12, Dec. 2017, Art. 2823.
- [19] B. R. Lavoie, M. Okoniewski, and E. C. Fear, “Optimizing Microwave-Radar Imaging Parameters,” in *Proceedings of the 17th International Symposium on Antenna Technology and Applied Electromagnetics (ANTEM)*, Montréal, QC, Canada: IEEE, Jul. 2016.
- [20] B. L. Oliveira, D. O’Loughlin, M. O’Halloran, *et al.*, “Microwave Breast Imaging: Experimental tumour phantoms for the evaluation of new breast cancer diagnosis systems,” *Biomedical Physics & Engineering Express*, vol. 4, no. 2, Feb. 2018, Art. 025036.
- [21] C. J. D’Orsi, E. B. Mendelson, and D. M. Ikeda, *Breast Imaging—Reporting and Data System*, 5th. Reston, VA, USA: American College of Radiology, 2013.
- [22] B. L. Oliveira, M. O’Halloran, R. C. Conceição, *et al.*, “Development of Clinically-Informed 3D Tumor Models for Microwave Imaging Applications,” *IEEE Antennas and Wireless Propagation Letters*, vol. 15, pp. 1–1, 2015.
- [23] H. Bahramiabarghouei, E. Porter, A. Santorelli, *et al.*, “Flexible 16 Antenna Array for Microwave Breast Cancer Detection,” *IEEE Transactions on Biomedical Engineering*, vol. 62, no. 10, pp. 2516–2525, Oct. 2015.
- [24] M. Klemm, I. J. Craddock, A. W. Preece, *et al.*, “Evaluation of a hemi-spherical wideband antenna array for breast cancer imaging,” *Radio Science*, vol. 43, no. 6, pp. 1–15, Dec. 2008.
- [25] D. O’Loughlin, M. A. Elahi, E. Porter, *et al.*, “Open-source software for microwave radar-based image reconstruction,” in *Proceedings of the 12th European Conference on Antennas and Propagation (EuCAP)*, London, the UK: IEEE, Apr. 9–13, 2018.
- [26] A. Santos, C. Ortiz de Solórzano, J. J. Vaquero, *et al.*, “Evaluation of autofocus functions in molecular cytogenetic analysis,” *Journal of Microscopy*, vol. 188, no. 3, pp. 264–272, 1997.
- [27] M. J. Yaffe, J. M. Boone, N. Packard, *et al.*, “The myth of the 50-50 breast,” *Medical Physics*, vol. 36, no. 12, pp. 5437–5443, Dec. 1, 2009.